Design and implementation of a system for monitoring PH level in water

YUE HOU
MASTER´S THESIS
DEPARTMENT OF ELECTRICAL AND INFORMATION TECHNOLOGY
FACULTY OF ENGINEERING | LTH | LUND UNIVERSITY

Design and implementation of a system for monitoring PH level in water

Master's Thesis

By

Yue Hou

Department of Electrical and Information Technology
Faculty of Engineering, LTH, Lund University
SE-221 00 Lund, Sweden

Supervisor: Baktash Behmanesh

Examiner: Pietro Andreani

LUND UNIVERSITY

2024

Abstract

With the development of the global economy and human society, population growth and urbanization, water resources are becoming more and more important, and the monitoring of water resources is also crucial. Therefore, this article designed a system for monitoring PH level in water, and designed a wireless transmission system based on LoRa technology. According to the actual application requirements of the system, the hardware circuit includes Power supply management module, Variable gain amplifier module, Analog-to-Digital Converter, Microcontroller and LoRa communication module.

In the testing part, another system for collecting water pH and temperature with Bluetooth transmission function was tested. But in the end the PCB did not achieve the expected function. After research and analysis, it was discovered that a problem occurred during manufacture that caused the board not working properly.

Acknowledgments

This Master's thesis would not exist without the support and guidance of Lund University for supporting my studying through these two years and providing me the laboratory equipment for testing the circuit board.

Also, I want to thank my supervisor, Baktash Behmanesh for helping me to the right direction when I am lost and supporting me professionally and spiritually.

Last, I want to thank my parents for supporting me all the time. They've always been my guidance in life.

Contents

List of figures

List of tables

List of acronyms

PCB	Printed Circuit Board
LoRa	Long Range Radio Frequency
VLF	Very Low Frequencies
EHF	Extremely High Frequencies
Wi-Fi	Wireless Fidelity
LANs	Local Area Networks
BLE	Bluetooth Low Energy
IoT	Internet of Things
NB-IoT	Narrowband IoT
LPWAN	Low-power Wide Area Network
3GPP	3rd Generation Partnership Project
ADC	Analog-to-Digital Converter
VGA	Variable Gain Amplifier
DAC	Digital-to-Analog Converter
USART	Universal Synchronous Asynchronous Receiver Transmitter
GPIO	General-purpose Input/Output
HIS	High-Speed Interna
HSE	High-Speed External Oscillator
LSI	Low-Speed Internal Oscillator
LSE	Low-Speed External
PLL	Phase-Locked Loop
ISSI	Integrated Silicon Solution, Inc
SPI	Serial Peripheral Interface
MCU	Microcontroller Unit
AFE	Analog Front End
FPU	Float Point Unit
SMD	Surface Mount Device

Popular Science Summary

This thesis work is about designing a system for monitoring PH level in water. With the development of the global economy and human society, population growth and urbanization, water resources are becoming more and more important. How to sustainably develop, utilize and manage water resources has attracted great attention from governments around the world and they have taken a variety of effective measures to ensure water security. Among them, monitoring water quality is a top priority.

The system is with LoRa wireless communication module. LoRa is a radio frequency technology used for low-power, long-distance communication. It allows devices to achieve long-distance communication in different geographical environments. The coverage can reach several kilometers. It has strong penetration capabilities and it's suitable for urban, rural and industrial fields. And low power consumption makes it ideal for remote sensors and IoT devices even if battery power is required all the time.

1. Introduction

1.1 Project Background

Water is an important resource for human survival and one of the most important material resources which are indispensable for human survival and development. Adults are made up of 50% to 60% water, and for infants and young children, this proportion can be as high as 70%, as shown in Figure 1[1].

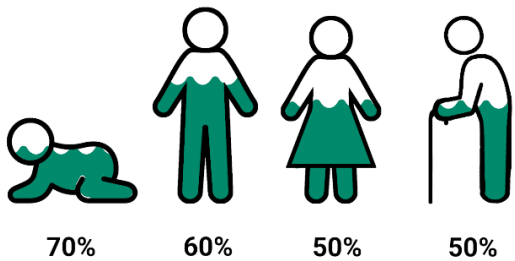

Fig. 1. Percentage of body made up of water

Water is the most important substance needed for human life, and almost all chemical reactions that occur in the body require the participation of water. It is an indispensable substance in the human body's metabolic process. It can promote metabolism, accelerate the absorption of nutrients and the discharge of waste in the body. Hence, maintaining water balance in the human body is an important part of maintaining health.

In addition to physical health, water is also important to humans in other aspects. It is estimated that globally, more than one billion jobs, which is more than 40% of the world's entire workforce, rely heavily on water resources, including agriculture, forestry, inland fisheries, mining and resource extraction, the energy industry, the health care industry, and multiple fields of light industry. There are also more than a billion jobs that are moderately dependent on water resources in heavy industries such as construction, entertainment, transportation, as well as heavy industries such

as rubber, plastics and metals. Therefore, building and maintaining water infrastructure, and providing related services such as water supply, wastewater treatment, etc., can provide a conducive working environment for the vast majority of people in the global economy.

With the development of the global economy and human society, population growth and urbanization, water resources are becoming more and more important. How to sustainably develop, utilize and manage water resources has attracted great attention from governments around the world and they have taken a variety of effective measures to ensure water security. Among them, monitoring water quality is a top priority. Among various parameters, pH value is essential. Therefore, in this thesis, we use Printed Circuit Board (PCB) to monitor the pH value of water.

In the early days of the development of water quality monitoring, most of the methods relied on manual on-site measurement. The inspectors needed to return to the required point to take samples again at regular intervals, and then brought them back to the laboratory for analysis and processing, and obtained a report. This method is time-consuming and laborious and cannot provide real-time data. With the development of electronic technology, in the mid-20th century, electronic sensors and automation equipment began to apply to water quality monitoring systems. This process makes monitoring more automated and real-time, reducing reliance on manual operations. In recent years, with the continuous development of Internet and communication technology, water quality monitoring systems have become more intelligent and interconnected. Modern water quality monitoring systems can transmit data through the Internet to achieve real-time monitoring, remote management and big data analysis.

Generally speaking, the development of water quality monitoring systems has experienced an evolution from manual operation to automation, from laboratory to field, from wired to wireless, and from local to global. This development process reflects the important role of scientific and technological progress in improving the accuracy, timeliness and operability of water quality monitoring.

1.2 Current status of water quality monitoring research

According to United States Environmental Protection Agency, the water quality parameter factsheets were developed to provide an introduction to monitoring common parameters; Temperature, Dissolved Oxygen, pH, Turbidity, Macroinvertebrates, E.coli, Nutrients, Habitat Assessment and Metals.

In order to monitor the parameters above better, the field of water quality monitoring is experiencing technological innovation rapidly. The development of new generation sensor technology, including miniaturization, high sensitivity and multi-parameter detection sensors, makes water quality monitoring more accurate and comprehensive. These sensors can monitor various water quality indicators in real time, such as pH, dissolved oxygen, turbidity, conductivity, etc. Using remote sensing technology from satellites, aircraft or drones, high-resolution images of large-scale water bodies can be obtained. These images can be used to monitor changes in water bodies, measure water body temperature, reflect water color, etc. Therefore, drone and satellite technology can be used for large-scale and remote water monitoring. The development of Internet has promoted the interconnection of water quality testing equipment. Various sensors and monitoring equipment can be connected in real time through the Internet to form an integrated water quality monitoring network to facilitate centralized management and analysis of data. Also, more analysis of water quality monitoring data can be performed by applying artificial intelligence and machine learning algorithms. This includes anomaly detection, predictive models and data pattern recognition to help understanding water body conditions better.

Countries around the world also have different characteristics in water body monitoring. Sensor technology is widely used in the United States to monitor water parameters such as temperature, pH, conductivity, and dissolved oxygen, as shown in Figure 2[2].

At the same time, advanced remote sensing technologies, such as satellites and drones, are also used to monitor water quality, shown in Figure 3[3].

Fig. 2. Different kinds of water quality sensors

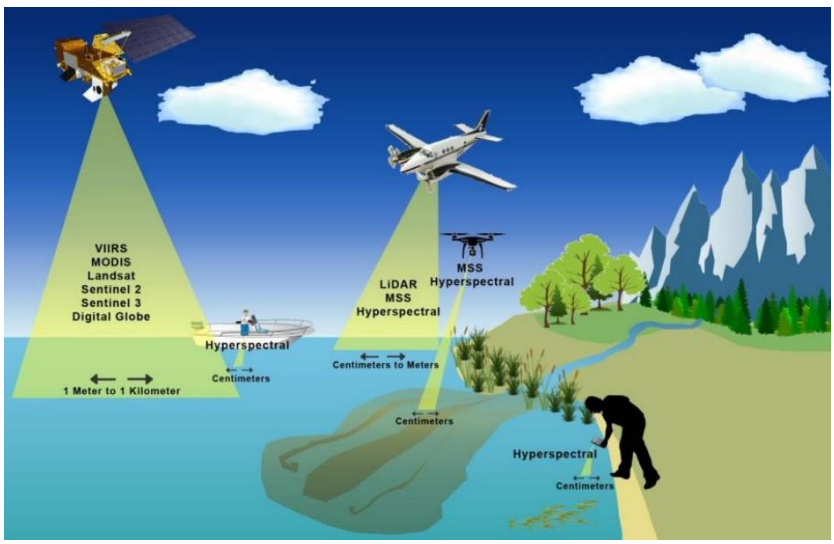

Fig. 3. Remote sensing technologies in water quality monitoring

European countries tend to adopt comprehensive water quality monitoring systems, including sensor technology, laboratory analysis, biological monitoring, etc. In China, in addition to the extensive use of sensor technology, a large number of water quality monitoring stations have also been built to monitor various parameters of water bodies. At the same time, a nationwide water quality monitoring network was implemented to conduct water quality assessment through big data analysis. Japan uses a highly

automated water quality monitoring system to monitor water conditions through real-time sensors.

1.3 Structure of the Thesis

According to the research above, this thesis presents a design and implementation of a system for monitoring PH level in water based on PCB and wireless communication technology.

Chapter 1 is Introduction, which introduces the project background and current status of water quality monitoring research.

Chapter 2 is Overall system design and related technology introduction. This chapter analyzes system design requirements from different aspects. It also introduces the related technologies of system design, mainly focusing on communication methods. This part introduces commonly used wireless communication technologies and their respective advantages and disadvantages, and selects the Long Range Radio Frequency (LoRa) according to system requirements.

Chapter 3 is Overall system design. This chapter completes the overall system design based on the system design requirements in Chapter 2. This chapter details the selection of important module chips and the circuit design details of each module. Finally, the circuit design of the system is completed.

2. Overall system design and related technology introduction

2.1 System design requirements

In order to solve the problem that some remote waters are difficult to access when monitoring the pH value of water bodies, this thesis uses PCB technology to build a system for monitoring the pH value in water. The PCB system has good reliability and can work stably for a long time, which includes properties such as resistance to high temperatures, humidity, and chemical corrosion. At the same time, it can also be highly integrated through printing technology to realize the design of complex electronic systems. This helps reduce the size and weight of electronic equipment and makes system installation easier. The PCB system is cheap, cost-effective, and easy to put into mass production. At the same time, the system is also equipped with LoRa, a low-power, long-distance, wide-area wireless communication technology for data transmission.

The system design requirements analysis is as follows:

1. System stability

Monitoring the pH value of water bodies may face some challenges, including complex and changeable environments, including temperature changes, physical vibrations and air state changes caused by weather changes, biological activities in water bodies, etc. Therefore, it is necessary to use a stable system with anti-interference performance.

2. Low power consumption of the system

Because the system needs to be located in remote, inaccessible waters, it needs to operate on battery power for extended periods of time. The low-power design can extend the running time of the water quality monitoring system and reduce the frequency of battery replacement. At the same time, it can reduce operating costs, reduce power consumption, and extend the service life of equipment, thereby improving the cost-effectiveness of the entire system.

3. Remote wireless data transmission

Through wireless transmission, water quality monitoring systems can transmit data in real time, which is crucial for timely detection of water body anomalies, handling pollution incidents, or making emergency decisions. Wireless transmission also adapts to different terrain and environmental conditions, especially in remote water scenarios that are difficult to access, wireless transmission provides stronger adaptability.

4. Easy to install and cost-effective

Using PCB technology to design a system, electronic components can be integrated on a flat board. The integrated design of the circuit helps reduce the size and weight of the entire device, making the device easier to install and carry. PCB designs often feature standard interfaces and connectors, making the assembly and disassembly process easier. At the same time, PCB manufacturing usually adopts mass production, which greatly reduces the manufacturing cost of each circuit board. This makes PCBs very cost-effective in mass production.

2.2 Related technologies

Wireless communication is a technology that transmits information through wireless transmission media, such as electromagnetic waves, infrared rays or other wireless media. This communication method allows data transmission between devices without physical connection, and it's widely used in various fields. Wireless communication is mainly achieved through the propagation of electromagnetic waves in space. These electromagnetic waves range in frequency from very low frequencies (VLF) to extremely high frequencies (EHF) and include radio waves, microwaves and infrared rays. Mainstream wireless communication technologies include 5G, 4G LTE, Wi-Fi, Bluetooth, Zigbee, LoRa, NB-IoT, etc[4].

The 5th generation mobile network. often referred to as 5G, is the latest generation technology standard in the current mobile communication field. 5G aims to provide higher data transmission rates, lower latency and greater device connection density than previous generation technologies to support a wide range of application scenarios, including mobile communications, Internet of Things, industrial automation, etc. 4G LTE is the generation before 5G. It is still widely used[5].

Wireless Fidelity (Wi-Fi) is a technology used for wireless communications that enables devices to transmit data over short distances via wireless signals. Wi-Fi technology is commonly used to create local area networks (LANs), allowing devices to connect wirelessly to share data, Internet access and other applications. It has the characteristics of high data transmission and support for multiple devices[6].

The advantage of Wi-Fi is that it allows devices to communicate wirelessly without a physical connection, providing greater flexibility and convenience. Compared with laying a wired network, Wi-Fi deployment and maintenance costs are generally lower, especially in small areas. The disadvantage of Wi-Fi is that Wi-Fi signals are susceptible to interference from electronic devices, obstacles, and other wireless networks, which can cause unstable connections or reduced transmission speeds. Signal coverage is also very limited, which usually is only 50m to 70m.

Bluetooth is a short-range wireless communication technology used to transfer data and establish connections between devices. Bluetooth technology is mainly used to achieve short-range communication, usually around 10 meters. This makes Bluetooth particularly suitable for near-field communications between devices. Bluetooth communications primarily operate in the 2.4 GHz frequency band. The band is split into multiple channels to reduce interference[7].

The advantage of Bluetooth devices is that they generally have lower power consumption, which makes them more suitable for battery-powered mobile devices. The Bluetooth Low Energy (BLE) standard even further improves Bluetooth's energy efficiency. Bluetooth is a widely supported technology, with almost all modern mobile devices and many other types of devices supporting Bluetooth communications. The disadvantage is that the communication distance is too short, usually around 10m. And the transmission rate is relatively low. Bluetooth signals are susceptible to interference from physical obstacles and other wireless devices, which may cause an unstable connection or degraded signal quality.

Zigbee is a low-power, short-distance, low-data-rate wireless communication technology that operates in the 2.4 GHz frequency band. Zigbee is a communication protocol standard based on the IEEE 802.15.4 standard that focuses on establishing simple, economical and reliable

wireless communication between low-power devices. It is widely used in Internet of Things (IoT) devices, sensors and controllers[8].

The advantage of Zigbee is its low power consumption makes it very suitable for battery-powered devices and it can extend the service life of the device. Zigbee is relatively simple to implement, which helps reducing the manufacturing cost of the device, making it an economical choice for large-scale IoT devices. And it supports a variety of network topologies, including star, mesh and hybrid, making it adaptable to different needs in different application scenarios. The disadvantage is that Zigbee's data transfer rate is relatively low, usually between 20-250 kbps. The communication range is generally between 10 and 100 meters, and it is only suitable for short-range communication. At the same time, because Zigbee operates in the 2.4 GHz frequency band and shares the same spectrum with other wireless devices, it may be interfered by other devices, especially in crowded wireless environments.

LoRa is a radio frequency technology used for low-power, long-distance communication. It allows devices to achieve long-distance communication in different geographical environments. The coverage can reach several kilometers. It has strong penetration capabilities and it’s suitable for urban, rural and industrial fields. And low power consumption makes it ideal for remote sensors and IoT devices even if battery power is required all the time[9].

The advantage of LoRa is that it supports long-distance communication and can achieve a communication range of several kilometers to dozens of kilometers in different terrains and environments. This makes LoRa suitable for long-distance sensor networks in smart cities, agriculture, and other industry fields. LoRa allows the creation of wide-area networks with long transmission distances. At the same time, the signal has strong penetrating capabilities and it can adapt to the crossing of buildings, trees and other objects, allowing it to provide better coverage in different environments. The disadvantage is that LoRa has lower data transfer rates, typically between 0.3 kbps and 50 kbps. This may limit its suitability in certain applications requiring high-speed data transmission. LoRa communication is generally not suitable for applications with high real-time requirements, such as real-time voice or video transmission, because its design focuses on low power consumption rather than high-speed real-time communication.

Narrowband IoT (NB-IoT) is a wireless communication technology that provides connectivity to IoT devices. It is a low-power wide area network (LPWAN) technology defined by the 3rd Generation Partnership Project (3GPP) and it's specifically designed to connect large numbers of low-power devices[10].

The advantage of NB-IoT is that it has wide coverage and can provide reliable communication services in various environments such as urban, rural and indoor environments. It also focuses on providing low-power communication, and it is suitable for IoT devices that require long-life battery power, thereby extending the service life of the device. NB-IoT use advanced encryption and authentication mechanisms to provide relatively high security and protect communication data from unauthorized access. The disadvantage is that compared to some other wireless technologies, NB-IoT has a lower data transmission rate, usually between 100 bps and 250 kbps, so it is not suitable for applications that require high-speed data transmission. The spectrum use of NB-IoT is regulated and managed and may be limited by spectrum resources, especially in some areas with limited spectrum resources. Another disadvantage is the initial cost of NB-IoT equipment is relatively high.

Among them, those that can be integrated on PCB include Bluetooth, Zigbee, LoRa and NB-IoT. Their comparison in various aspects is shown in Table 1.

Generally speaking, wireless communication technology follows the rule that the higher the communication rate, the farther the communication distance. The communication distance is directly related to the transmit power of the wireless radio frequency module, resulting in the power consumption of the device increasing as the distance increases. However, LoRa technology can maintain a large communication distance with low power consumption. The slight disadvantage is that the data transmission rate is relatively low. Therefore, LoRa is suitable for areas that have higher requirements for network coverage and low power consumption but lower transmission rates, and it perfectly matches the application scenarios of the required systems[11].

Performance	Bluetooth	Zigbee	LoRa	NB-IoT
Communication distance	10m	100m	5 km	10 km
Data rate	1Mbps-2Mbps	250Kbps	5Kbps	20 kbps
Power consumption	Low	Low	Low	Low
Frequency band	2.4 GHz	2.4 GHz, 868 MHz, 915 MHz	433MHz, 868MHz, 915MHz.etc	Mainly in the LTE band
Cost	relatively low	Medium	Medium to low	Medium to low
battery power	Need	Need	Need	Need
Data encryption	WPA3 support	AES Encryption and Authentication	AES Encryption and Authentication	Encryption and Authentication

Table 1. Comparison in various aspects of different communication methods

3. Overall system design

This chapter focuses on the system hardware design and the principles and implementation process of each functional module circuit. The system for monitoring PH level in water uses STM32L476ZET6 as the control core and uses the SX1278 radio frequency chip to achieve wireless data transmission. According to the overall system design plan, the system includes a power supply management module, a variable gain amplifier module, an Analog-to-Digital Converter (ADC) module, a microcontroller module, a LoRa wireless communication module and an external memory. The analog signal received from the pH sensor enters the amplifier for amplification, then enters the ADC to be converted into a digital signal, and then enters the microcontroller STM32L476ZET6 for processing. The processed data will be stored in external memory or transmitted by the SX1278 radio frequency chip in LoRa wireless communication mode.

3.1 Overall system framework

The core of the system is a microcontroller, and the STM32L476ZET6 microcontroller is selected. The power supply management module uses LM79L05 chip and AMS1117 chip for voltage controlling, converting from 6V supply voltage to 5V and from 5V supply voltage to 3.3V respectively. Since the required amplifier gain is an unconventional value, the variable gain amplifier AD8367 was selected. ADC uses AD7478. The wireless communication module uses SX1278. IS62WV51216 is for external memory. Figure 4 is the overall framework of the system.

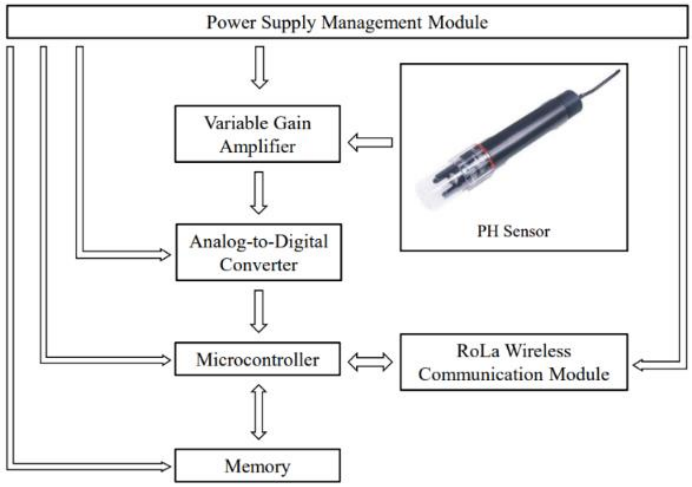

Fig. 4. Overall system framework

3.2 Power supply management module

The pH value monitoring system designed in this thesis consists of multiple modules, and their power supply voltages are not exactly the same. In order for each module to work properly, this thesis needs to provide 5V and 3.3V power supply voltages. Power supplies with a 5V supply voltage cannot be purchased directly, so in order to make the system more portable, among the common batteries that provide 6V and 12V voltage, we use the 6V supply voltage battery which is smaller. This article uses LM79L05 to convert 6V to 5V, and uses AMS1117 to convert 5V to 3.3V. The voltage controlling circuit design is shown in Figure 5[12].

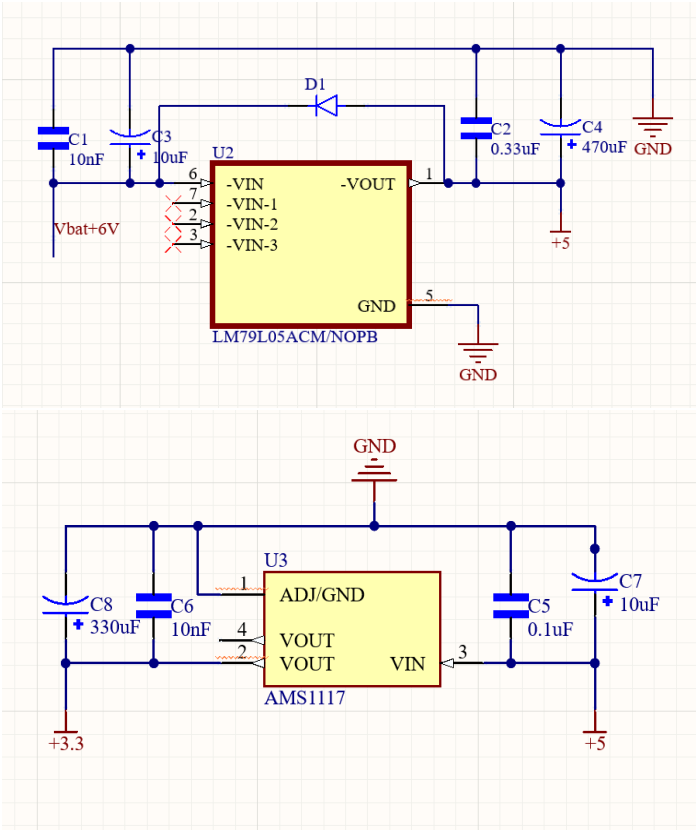

Fig. 5. The voltage controlling circuit

3.3 Variable gain amplifier module

Since the analog signal collected from the pH sensor does not exactly match the voltage that the ADC can receive, the analog signal collected by the pH sensor needs to be amplified through an amplifier. According to the datasheets, the analog signal output of the PH sensor is from 0V to 2V, and the input voltage of the ADC is from 0.4V to 2.4V. It can be seen that the required gain is not a fixed value. Therefore, this thesis chooses the variable gain amplifier AD8367 to process the signal.

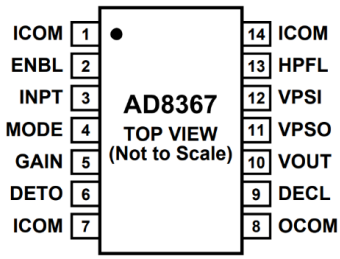

Fig. 6. Pin Configuration of AD8367

The AD8367 is a general-purpose Variable gain amplifier (VGA) suitable for use in a wide variety of applications where voltage control of gain is needed. Figure 6 is the Pin Configuration of AD8367. Table 2 shows the Pin Function Descriptions of AD8367 according to the datasheet.

Pin No.	Mnemonic	Description
1, 7, 14	ICOM	Signal Common. Connect to low impedance ground.
2	ENBL	A HI Activates the Device.
3	INPT	Signal Input. 200 Ω to ground.
4	MODE	Gain Direction Control. HI for positive slope; LO for negative slope.
5	GAIN	Gain Control Voltage Input.
6	DETO	Detector Output. Provides output current for RSSI function and AGC control.
8	OCOM	Power Common. Connect to low impedance ground.
9	DECL	Output Centering Loop Decoupling Pin.
10	VOUT	Signal Output. To be externally ac-coupled to load.
11	VPSO	Positive Supply Voltage. 2.7 V to 5.5 V. VPSI and VPSO are tied together internally with back-to-back PN junctions. They should be tied together externally and properly bypassed.
12	VPSI	Positive Supply Voltage. 2.7 V to 5.5 V.
13	HPFL	High-Pass Filter Connection. A capacitor to ground sets the corner frequency of the output offset control loop.

Table 2. Pin Function Descriptions of AD8367

In this thesis, we choose to use Voltage Controlled Gain Mode connections. Figure 7 is basic connections for Voltage Controlled Gain Mode. The C_{HP} capacitor at Pin HPFL can be used to alter the high-pass corner frequency of the signal path and is associated with the offset control loop that eliminates the inherent variation in the internal dc balance of the signal path as the gain is varied (offset ripple), and an internal network provides a default high-pass corner of about 500 kHz.

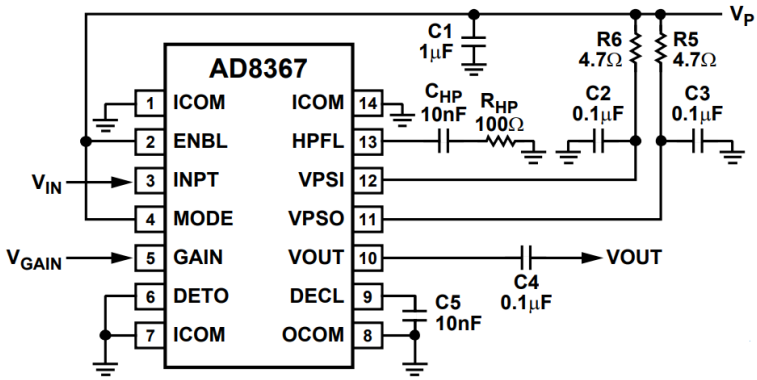

Fig. 7. Basic Connections for Voltage Controlled Gain Mode

When V_S = 5 V, T_A = 25°C, system impedance Z_O = 200 Ω, V_{MODE} = 5 V, the relationship between Gain, frequency and V_{GAIN} is shown in Figure 8. It can be seen from the figure that when the system works normally, the required V_{GAIN} is between 0.1V and 0.2V.

This thesis uses ordinary resistor R13 and variable resistor R12 to change the voltage division control V_{GAIN}, thereby changing the gain, as shown in Figure 9.

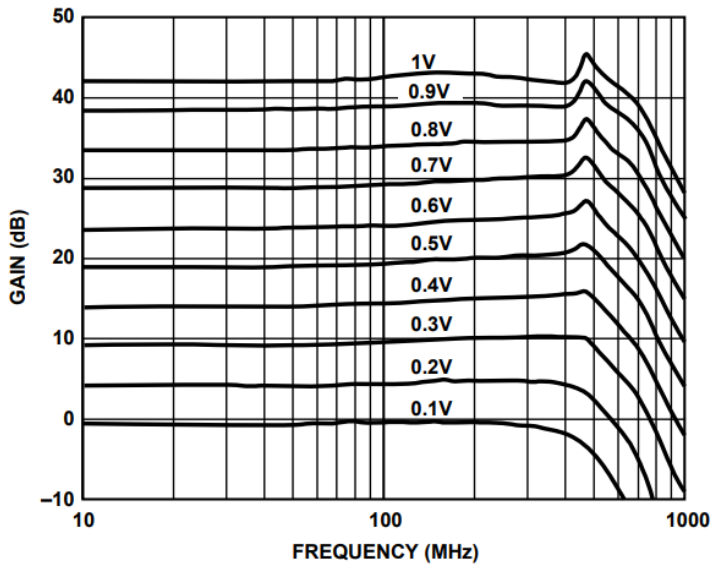

Fig. 8. Gain vs. Frequency for Values of V_{GAIN}

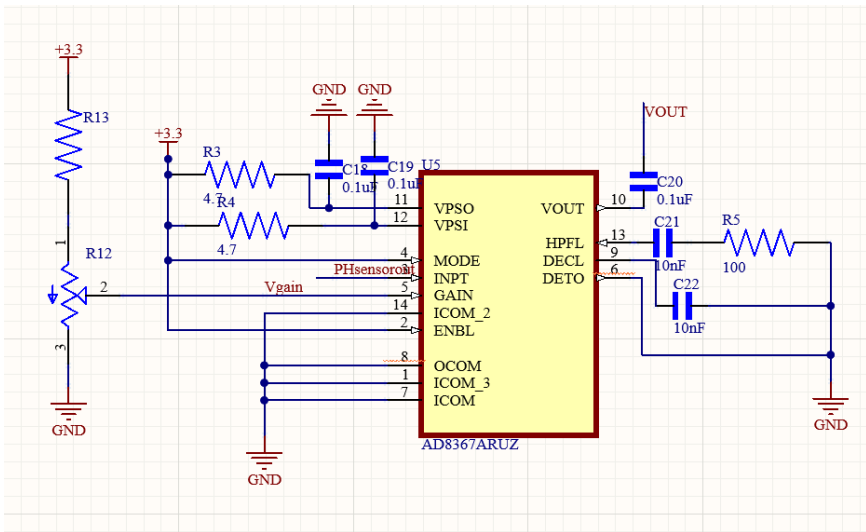

Fig. 9. Controlling V_{GAIN} through a variable resistor

3.4 Analog-to-Digital Converter

This system only requires the pH value of the obtained data and does not have high accuracy requirements. Therefore, sacrificing data accuracy in exchange for more data volume is one of the needs. Therefore, 8-bit ADC is enough. ADC AD7478 is selected. AD7478 is 8-bit, high speed, low power, successive approximation ADC. Figure 10 is the Pin Configuration of AD7478. Table 3 shows the Pin Function Descriptions of the AD7478 according to the datasheet.

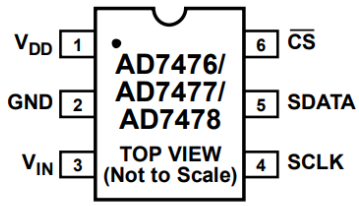

Fig. 10. Pin Configuration of AD7478

Pin No.	Mnemonic	Description
1	V_{DD}	Power Supply Input.
2	GND	Analog Ground. Ground reference point for all circuitry on the part.
3	V_{IN}	Analog Input. Single-ended analog input channel.
4	SCLK	Serial Clock. Logic input.
5	SDATA	Data Out. Logic output. The conversion result is provided on this output as a serial data stream.
6	$\overline{CS}$	Chip Select. Active low logic input.

Table 3. Pin Function Descriptions of AD7478

3.5 Microcontroller

3.5.1 Microcontroller Selection

With continuous development of the chip field, the iteration of microcontrollers is changing with each passing day, and the range of options is increasing. Choosing the right microcontroller is critical to the success of projects. The choice of microcontroller involves many aspects, including project needs, performance requirements, power consumption, cost, etc. Currently widely used microcontrollers include STM32 Family, AVR Family, MSP430 Family, nRF52 Family, LPC Family, PSoC Family, etc. The performance comparison of these microcontrollers is shown in Table 4.

Microcontroller type	Processing Power	Functions	Power Consumption	Price	Communication Interfaces
STM32 Family	High	Complete	Relatively Low	Medium	Multiple, Large quantity
AVR Family	Low-Medium	Relatively incomplete	Relatively Low	Low-Medium	Basic, Small quantity
MSP430 Family	Low	Relatively incomplete	Low	Low-Medium	Basic, Small quantity
nRF52 Family	Medium	relatively complete	Relatively Low	Medium	Mainly Bluetooth, Large quantity
LPC Family	Medium-High	relatively complete	Relatively Low	Medium-High	Multiple, Large quantity
PSoC Family	Medium	Complete	Low	Low-Medium	Multiple, Large quantity

Table 4. Microcontroller performance comparison

Based on the comprehensive comparison in the above table, this thesis determines to choose the STM32 Family of STMicroelectronics. The Family features high performance, lower cost and low power consumption. Compared with AVR and MSP430, STM32 is more powerful, it has more communication interfaces, and it can support a variety of mainstream operating systems. Compared with LPC and PSoC, STM32 has stronger processing power, and it is easier to operate, so that more friendly to

beginners. The communication interface of nRF52 is mainly Bluetooth, which is not consistent with the LoRa used in this system. After comprehensive consideration, the STM32 Family is more suitable for the needs of this system.

Among them, STM32L476ZET6 is one of the low-power microcontroller series STM32L476 launched by STMicroelectronics. It is based on the ARM Cortex-M4 core and has 144 pins, including up to 114 GPIO pins, which can meet the needs of this design. The actual object is shown in Figure 11.

Fig. 11. Physical picture of STM32L476ZET6

The following are some product parameters of this microprocessor:

1. Operating Voltage: From 1.71 V to 3.6 V
2. Temperature range: From -40°C to +85°C
3. Memory: 512 KB Flash memory and 128KB RAM
4. Operating Frequency: Up to 80 MHz
5. Core: ARM Cortex-M4 processor
6. Peripheral Interfaces: Multiple USART, SPI, I2C interfaces for communication and USB interface for connectivity
7. Package Type: LQFP144(20*20)

8. Security Features: Hardware encryption engine for secure data transmission and Secure storage options to protect sensitive information

STM32L476ZET6 is a high-performance microcontroller with rich on-chip resources, 144 package pins and 512KB flash memory. In terms of peripherals, it has three 12-bit ADCs and two 12-bit Digital-to-Analog Converters (DAC), providing powerful peripheral support for the system. STM32L476ZET6 has a flexible clock system that allows users to configure different clock sources and frequencies. These include:

1. High-Speed Internal (HIS) oscillator. Typical frequency is 16MHz.
2. High-Speed External (HSE) oscillator. It can be connected to the chip's crystal oscillator.
3. Low-Speed External (LSE) oscillator. Typically used to provide low power clocks.
4. Low-Speed Internal (LSI) oscillator. Typically used to provide a clock when it is in low power modes.
5. Phase-Locked Loop (PLL). Allows the user to generate a high frequency clock source by multiplying or dividing the input clock. This is useful for applications requiring higher clock speeds.

3.5.2 STM32 communication interfaces

Serial communication of STM32 microcontrollers usually uses the Universal Synchronous Asynchronous Receiver Transmitter (USART). USART is a universal serial communication interface that can operate in synchronous or asynchronous mode. In STM32 microcontrollers, the USART is usually used for serial communication. It supports full-duplex communication, allowing simultaneous transmission and reception of data. Figure 12 is the functional block diagram of USART[13].

Here are some of the key features and parameters of USART:

1. Baud Rate: Baud Rate is an important parameter in USART communication, indicating the number of bits transmitted per second. Both ends of the communication must be set to the same baud rate to transmit data correctly.

2. Frame Format: USART supports different frame formats, including data bit length, stop bits, and parity bits. Common data bit lengths are 8 bits, stop bits are 1 bit, and parity checking is usually disabled.
3. Synchronous and asynchronous modes: USART can work in synchronous mode or asynchronous mode. In asynchronous mode, start and stop bits are used to synchronize data, while in synchronous mode, synchronization is done by an external clock signal.
4. Mode: USART usually has different modes, including full-duplex mode, half-duplex mode, etc. In full-duplex mode, data can be sent and received simultaneously.

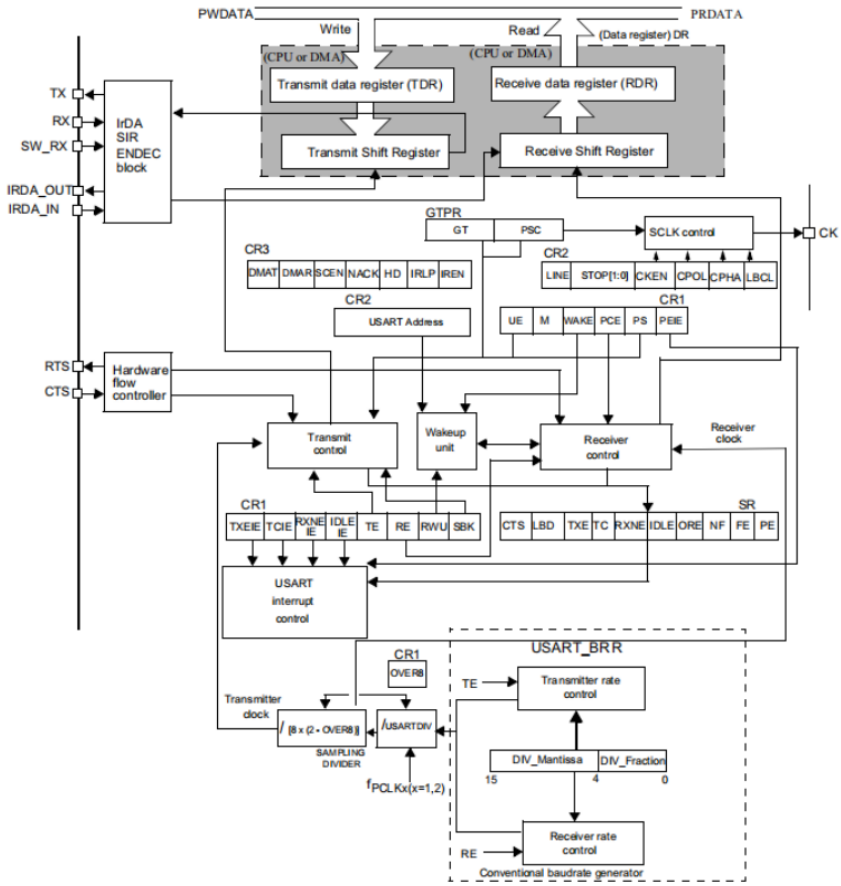

Fig. 12. Functional block diagram of USART

The basic steps for using USART for serial communication on STM32 are as follows:

1. Configure the GPIO interfaces and connect them with the transmit (TX) and receive (RX) pins of the USART module.
2. Initialize the USART module and set parameters such as baud rate and frame format.
3. Use HAL library or underlying driver to send and receive data.

The communication interfaces of STM32 include:

1. TX: Transmit interface. Where the device sends out data.
2. RX: receiving interface. Where the device receives incoming data.
3. SW_RX: The data receiving interface, which is only used in single-line and smart card modes. It is an internal pin and has no specific external pin.
4. nRTS: Request to Send. 'n' means active low. If RTS flow control is enabled, nRTS will be set low when the USART receiver is ready to receive new data; nRTS will be set high when the receive register is full. This pin is only available for hardware flow control.
5. nCTS: Clear to Send. 'n' means active low. If CTS flow control is enabled, the transmitter will detect the nCTS pin before sending the next frame of data. If it is low level, it means that data can be sent. If it is high level, it will stop sending after sending the current data frame. This pin is only available for hardware flow control.
6. SCLK: Transmitter clock output pin. This pin is only available in synchronous mode.

The specific distribution of USART pins in STM32L476ZET6 is shown in Table 5.

Pin	APB2 Bus	APB1 Bus	
	USART1	USART2	USART3
TX	PA9	PA2	PC10
RX	PA10	PA3	PC11
SCLK	PA8	PA4	PC12
nRTS	PA12	PA1	PB1
nCTS	PA11	PA0	PB0

Table 5. The specific distribution of USART pins in STM32L476ZET6

3.5.3 Reset Circuit

The reset circuit can restore most registers to their original state, that is, allowing the program to restart reset operation. The principle of the reset circuit is that when power is turned on, the current charges the capacitor through the resistor and capacitor. At this time, the reset pin is at low level. After pressing the reset button, the capacitor begins to discharge, causing the reset pin voltage to gradually increase from low level until it reaches high level, thereby completing the reset of the microcontroller. Reset Circuit is shown in Figure 13.

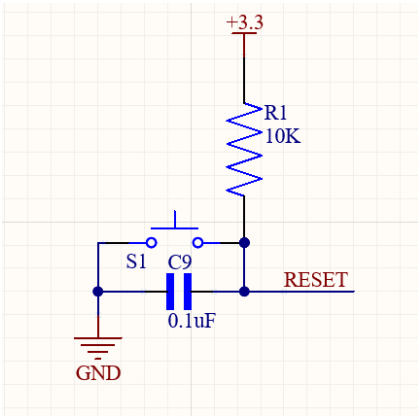

Fig. 13. Reset Circuit

3.5.4 Clock Circuit

The crystal oscillator provides a stable working clock signal for the system to ensure the orderly and stable operation of the system. There are 5 types of clock signals for STM32L476ZET6. In actual use, HSE is generally selected as the clock source of the external system. The optional frequency of the external crystal oscillator is 4~16MHz. The frequency used in this design is 8MHz. RTC real-time clock generally uses LSI (Low-Speed Internal oscillator), because 2 to the 15th power is equal to 32768, that is, 32768 is exactly 1 after being divided by 15. Therefore, the external crystal oscillator

frequency of this design is 32.768kHz. The clock circuit is shown in Figure 14 and Figure 15[14].

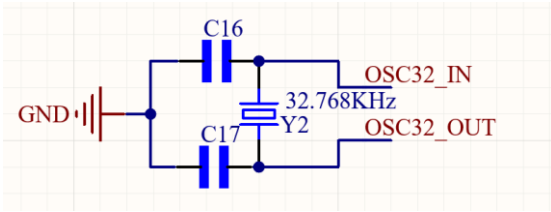

Fig. 14. 32.768kHz crystal oscillator clock circuit

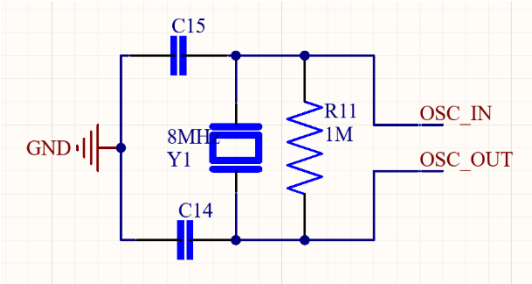

Fig. 15. 8MHz crystal oscillator clock circuit

3.6 Memory

Although STM32L476ZET6 has built-in 512 KB Flash memory and 128KB RAM, they still cannot meet the system's data storage needs. Therefore, the system requires additional external memory. The SRAM used in this thesis is IS62WV51216, which is a 16-bit wide 1 Mbyte capacity CMOS static memory chip produced by Integrated Silicon Solution (ISSI), Inc. The pin diagram is shown in Figure 16.

The addressing space of address lines A0 to A18 is 512K. Because the data width is 16 bits or two bytes, 512K*2Byte = 1MB capacity. The function of LB and UB is to control the data validity of high and low bytes. The truth table of IS62WV51216 is shown in Table 7.

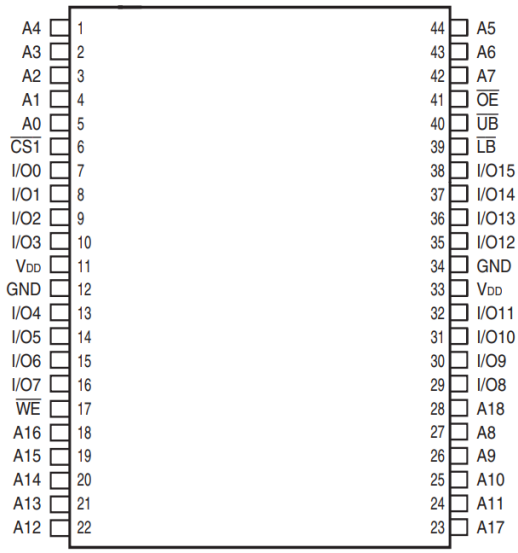

Fig. 16. Pin Configuration of IS62WV51216

Pin Descriptions are shown in Table 6.

Mnemonic	Description
A0-A18	Address Inputs
I/O0-I/O15	Data Inputs/Outputs
$\overline{CS1}$, CS2	Chip Enable Input
$\overline{OE}$	Output Enable Input
$\overline{WE}$	Write Enable Input
$\overline{LB}$	Lower-byte Control (I/O0-I/O7)
$\overline{UB}$	Upper-byte Control (I/O8-I/O15)
NC	No Connection
V_{DD}	Power
GND	Ground

Table 6. Pin Descriptions of IS62WV51216

							I/O PIN		
Mode	$\overline{WE}$	$\overline{CS1}$	CS2	$\overline{OE}$	$\overline{LB}$	$\overline{UB}$	I/O0-I/O7	I/O8-I/O15	V_{DD} Current
Not Selected	X	H	X	X	X	X	High-Z	High-Z	I_{SB1}, I_{SB2}
	X	X	L	X	X	X	High-Z	High-Z	I_{SB1}, I_{SB2}
	X	X	X	X	H	H	High-Z	High-Z	I_{SB1}, I_{SB2}
Output Disabled	H	L	H	H	L	X	High-Z	High-Z	I_{CC}
	H	L	H	H	X	L	High-Z	High-Z	I_{CC}
Read	H	L	H	L	L	H	D_{OUT}	High-Z	I_{CC}
	H	L	H	L	H	L	High-Z	D_{OUT}	
	H	L	H	L	L	L	D_{OUT}	D_{OUT}	
Write	L	L	H	X	L	H	D_{IN}	High-Z	I_{CC}
	L	L	H	X	H	L	High-Z	D_{IN}	
	L	L	H	X	L	L	D_{IN}	D_{IN}	

Table 7. The truth table of IS62WV51216

3.7 LoRa communication circuit

3.7.1 RFIC selection

This section selects chips based on the previous requirements analysis. Widely used frequency bands in low-power wide area networks include 315MHz, 433MHz, 470-510MHz, 868MHz, 915MHz, etc., which can be collectively referred to as Sub-1GHz. At present, the RF ICs in the Sub-1GHz band mainly include TI's CC1125, Silicon Lab's Si4432 and Si4438, Semtech's SX1278, Analog Devices' ADF7023, etc. The performance comparison of these products is shown in Table 8[15].

Considering various aspects of transmission distance, low power consumption and communication reliability, as well as miniaturization, simplicity, scalability and other factors, this design finally chooses the sub-1GHz low-power wireless radio frequency transceiver chip SX1278 produced by Semtech, based on LoRa spread modulation technology.

RFIC	CC1125	Si4432	Si4438	SX1278	ADF7023
Frequency Band/MHz	315/433/915	240-930	425-525	433/470	431-464/862-928
Modulation Scheme	FSK/GFSK	GFSK	GFSK/ OOK	LoRa	FSK/GFSK/OOK
Sensitivity/dBm	-129	-121	-124	-132	-116
Maximum Data Rate/kbps	200	500	500	300	300
Transmit Power/dBm	+16	+20	+20	+20	+13.5
Receive Current/mA	17	18.5	14	9.9	5
Communication Range/km	2	1.8	1.8	5	1.8

Table 8. Performance comparison of different RFICs

Center frequency of SX1278 includes 433MHz, 470MHz, etc., and the communication distance can reach up to 5km. The output power is usually between +5dBm and +20dBm and it can be adjusted as needed. Data rates are configurable and typically range from 300 bps to 37.5 kbps.

3.7.2 Pin Description of SX1278

Figure 17 shows the Pin Diagram of SX1278.

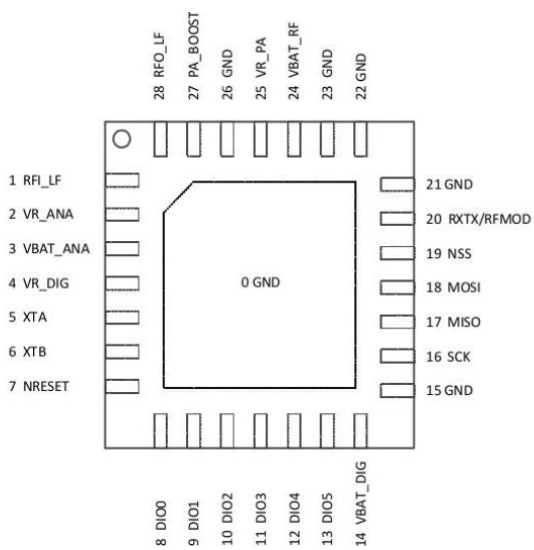

Fig. 17. Pin Diagram of SX1278

The Pin Function Description of SX1278 is shown in Table 9.

Pin No.	Mnemonic	Description
0	GROUND	Exposed ground pad
1	RFI_LF	RF input for bands 2&3
2	VR_ANA	Regulated supply voltage for analogue circuitry
3	VBAT_ANA	Supply voltage for analogue circuitry
4	VR_DIG	Regulated supply voltage for digital blocks
5	XTA	XTAL connection or TCXO input
6	XTB	XTAL connection
7	NRESET	Reset trigger input
8	DIO0	Digital I/O, software configured
9	DIO1/DCLK	Digital I/O, software configured
10	DIO2/DATA	Digital I/O, software configured
11	DIO3	Digital I/O, software configured
12	DIO4	Digital I/O, software configured
13	DIO5	Digital I/O, software configured
14	VBAT_DIG	Supply voltage for digital blocks
15	GND	Ground
16	SCK	SPI Clock input
17	MISO	SPI Data output
18	MOSI	SPI Data input
19	NSS	SPI Chip select input
20	RXTX/RF_MOD	Rx/Tx switch control: high in Tx
21	RFI_HF (GND)	RF input for band 1 (Ground)
22	RFO_HF (GND)	RF output for band 1 (Ground)
23	GND	Ground
24	VBAT_RF	Supply voltage for RF blocks
25	VR_PA	Regulated supply for the PA
26	GND	Ground
27	PA_BOOST	Optional high-power PA output, all frequency bands
28	RFO_LF	RF output for bands 2&3

Table 9. Pin Function Description of SX1278

3.7.3 LoRa circuit design

The SX1278 RF chip and its peripheral circuit are shown in Figure18. SX1278 adopts half-duplex communication method. The pins of SX1278 include GPIO pins, RF IO pins, serial Peripheral Interface (SPI) pins, power pins and ground pins. The 3rd pin VBAT_ANA is the radio frequency power supply, and the 14th pin VBAT_DIG is connected to the digital I/O power supply and is powered by 3.3V. A voltage protection circuit is formed by connecting a filter capacitor in parallel to reduce power supply ripple and maintain the stability of the power supply. DIO0-5 are terminal output pins, and their output is determined through programming. SX1278 can feedback the status to the Microcontroller Unit (MCU) through the status register and DIO0-5, and these 6 general-purpose IO pins can be used in LoRa communication mode. RFI-LF is a low frequency pin and RFI-HF is a high frequency pin. L2 and C31 form the filter of the receiving circuit, and C32 is the compensation capacitor of the low-pass filter. C42, L5 and C23, L76 form two sets of parallel resonant circuits of the transmitter circuit[16].

SX1278 and MCU communicate through SPI bus. The enable pin NSS of SX1278 is connected to the IO port PA4 of STM32 and it is active low. The reset pin NRESET is connected to PB0 of STM32 and it is active low. Four SPI buses (SCK, MISO, MOSI, NSS) are connected to PA5, PA6, PB5, and PA4 of STM32 respectively.

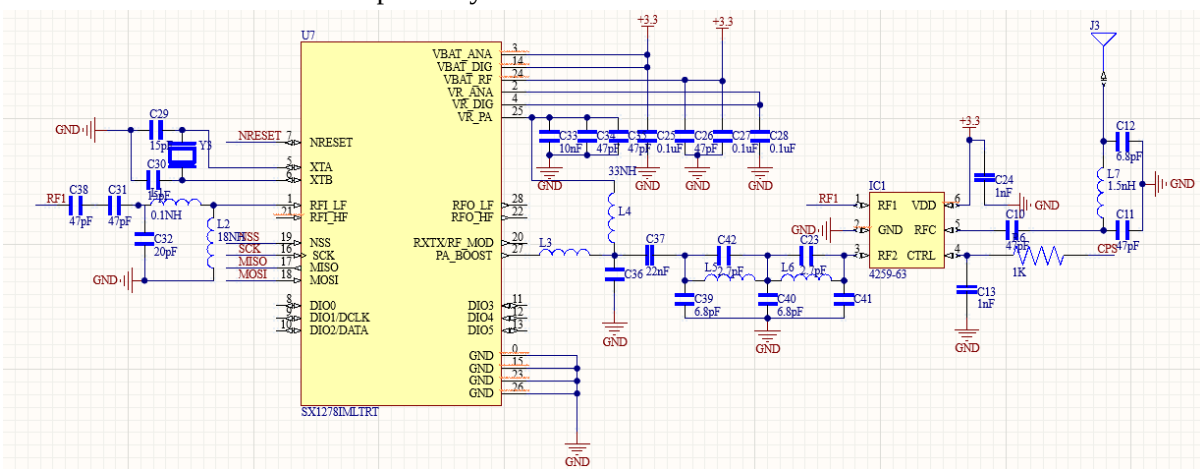

Fig. 18. SX1278 RF chip and its peripheral circuits

STM32 completes two-way communication with SX1278 through the SPI interface, where STM32 is the Master and SX1278 is the Slave. The MCU uses SPI to read the status information of SX1278. The data in the FIFO register of SX1278 relies on interrupts to read and write. The data transmission block diagram of STM32 and SX1278 is shown in Figure 19.

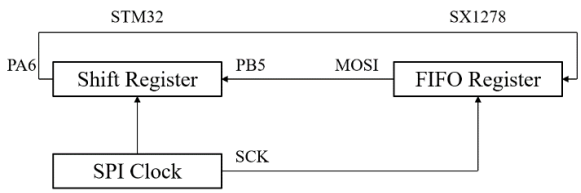

Fig. 19. The data transmission block diagram of STM32 and SX1278

The Master STM32 writes the data into the data register corresponding to its SPI, and starts shifting and sending according to the SPI timing of the hardware circuit. The data is sent to the MISO pin of the SX1278 through the I/O pin PA6 of the STM32, and then sent out by the SX1278 RF module. The data is sent one byte at a time. Only when all the data in the SPI register is moved out, a data exchange is completed.

Since there are many RF types in daily production and life, and radio frequency signals are sent and received through antennas, diverse and mutually interfering radio signals will interfere with the radio frequency module and reduce its sensitivity. In order to reduce the interference of other signals and because of its half-duplex working mode, the PE4259 switch chip is selected to complete the switching of signal sending and receiving and separate the sending and receiving branches. When transmitting a signal, switch the antenna to transmit mode. Otherwise, it switches to receiving mode.

4 Testing of new PCB

Because the production cost of this design in this thesis is too high and the manufacturing cycle is long, we did not choose to manufacture and test the design of this thesis in the testing process. Instead, we used the design of another graduate student that had already been manufactured. The function of this design is to measure and collect data on pH value and temperature of water bodies and transmit the data via Bluetooth.

But after various attempts and research, the test failed and the board did not achieve the expected functions. Therefore, this chapter will first introduce how the PCB is designed, and then introduce how I tested it and why I personally think the test failed.

4.1 Schematic of PCB design for testing

4.1.1 Power Supply

The power supply voltage in this design is all 3.3V, some devices have a reference voltage of 5V, and some devices have a reference voltage of 3.3V, so the power supply system needs to provide different voltages. At the same time, this system is used to measure the pH value and temperature of water bodies. It needs to operate independently in the water for a long time and has no external power supply, so it requires battery power. This design is also equipped with a charging device, which will automatically charge when the USB is connected to the PCB.

USB adapter battery charger circuit is shown in Figure 20. MAX1555 can charge a single-cell lithium-ion (Li+) battery from both USB and AC adapter sources, enabling portable users to forgo carrying a wall cube. These devices operate with no external FETs or diodes, and accept operating input voltages up to 7V.

The MAX1551/MAX1555 can charge from either the USB input or the DC input. The battery does not charge from both sources at the same time. With USB connected, but without DC power, the charge current is set to 100mA (max). This allows charging from both powered and unpowered USB hubs with no port communication required. When DC power is connected, charging current is set at 280mA (typ). The MAX1551/MAX1555 do not feature an enable input. Once power is

connected to USB and/or DC, the charger is on. Typically, V_{Bus} is 5V. The USB connector circuit is shown in Figure 21. The interfaces USB_P and USB_N are directly connected to the microcontroller. The Pin Function Description of MAX1555 is shown in Table 10.

In order to obtain the V_{ref} required in the PH sensor module from V_{Bat+}, REF3030 is used. The REF3030 is a precision, low-power, low-dropout voltage, reference. According to the datasheet, when the input voltage is 5V, the output voltage is 3V±0.006V. The circuit diagram of REF3030 is shown in Figure 22.

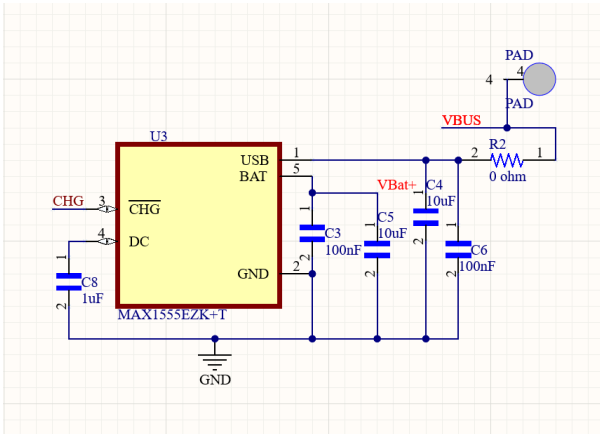

Fig. 20. USB adapter battery charger circuit

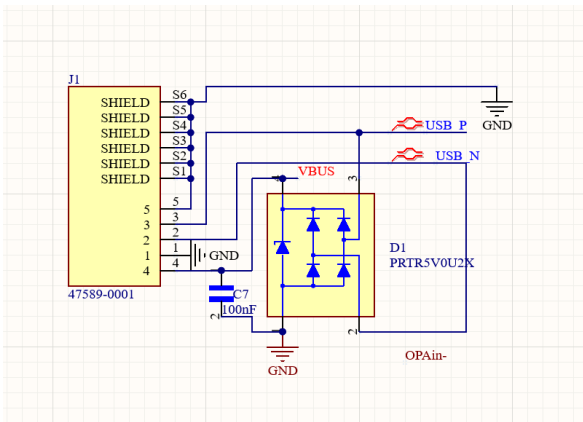

Fig. 21. USB connector circuit

Pin No.	Mnemonic	Description
1	USB	USB Port Charger Supply Input. USB draws up to 100mA to charge the battery. Decouple USB with a 1µF ceramic capacitor to GND
2	GND	GROUND
3	$\overline{CHG}$	Active-Low Open-Drain Charge Status Indicator. CHG pulls low when the battery is charging. CHG goes to a high-impedance state, indicating the battery is fully charged, when the charger is in voltage mode and charge current falls below 50mA. CHG is high impedance when both input sources are low (MAX1555 only)
4	DC	DC Charger Supply Input for an AC Adapter. DC draws 280mA to charge the battery. Decouple DC with a 1µF ceramic capacitor to GND.
5	BAT	Battery Connection. Decouple BAT with a 1µF ceramic capacitor to GND

Table 10. Pin Function Description of MAX1555

In order to obtain the V_{ref} required in the PH sensor module from V_{Bat+}, REF3030 is used. The REF3030 is a precision, low-power, low-dropout voltage, reference. According to the datasheet, when the input voltage is 5V, the output voltage is 3V±0.006V. The circuit diagram of REF3030 is shown in Figure 22.

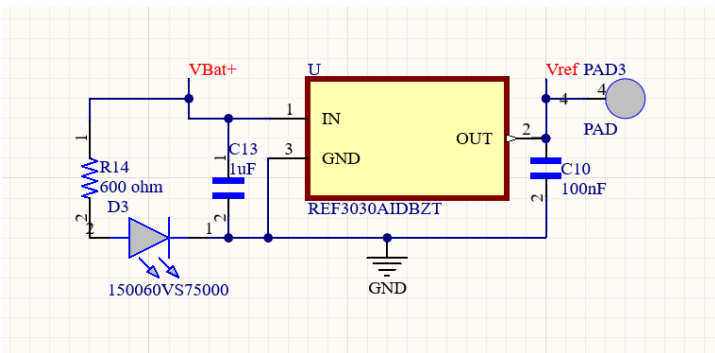

Fig. 22. Circuit Diagram of REF3030

To obtain a stable 3.3V voltage, voltage regulator TPS70366 is used. The circuit diagram is shown in Figure 23.

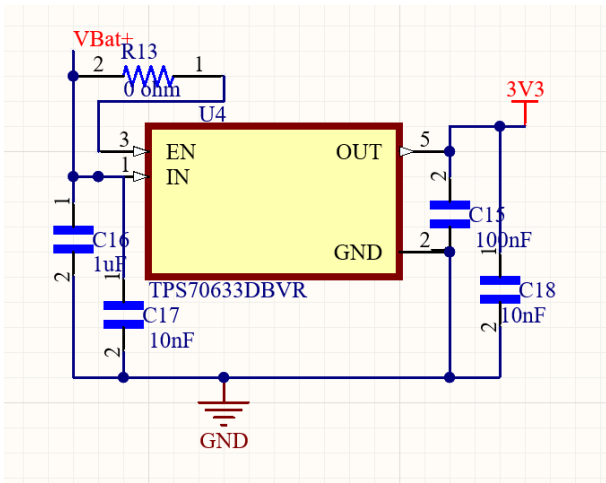

Fig. 23. Voltage Regulator TPS70366

4.1.2 PH Sensor and Temperature Sensor Platforms

The purpose of this design is to measure the PH value and temperature of the water body, so it is equipped with PH sensor and temperature sensor platforms.

PH sensor platform uses LMP91200, which is a sensor Analog Front End (AFE) for use in low-power, analytical-sensing applications. The LMP91200 is designed for 2-electrode sensors. This device provides all of the functionality needed to detect changes based on a delta voltage at the sensor. Optimized for low-power applications, the LMP91200 works over a voltage range of 1.8 V to 5.5 V. Circuit diagram of LMP91200 is shown in Figure 24.

The pin description is shown in Table 11. (D = Digital, A = Analog, P = Power, G = GND)

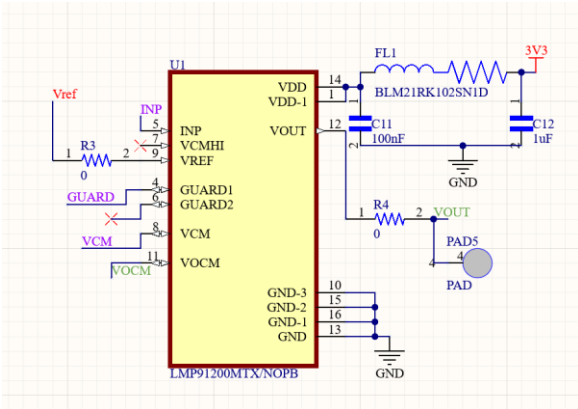

Fig. 24. Circuit Diagram of LMP91200

Pin No.	Mnemonic	Type	Description
1	VDD	P	Positive Power Supply
2	NC	A	No connect. These pins should be left floating
3	NC	A	No connect. These pins should be left floating
4	GUARD1	A	Active guard pin
5	INP	A	Noninverting analog input of pH buffer
6	GUARD2	A	Active guard pin
7	VCMHI	A	High Impedance Common-Mode output
8	VCM	A	Buffered Common-Mode output
9	VREF	A	Voltage reference input
10	GND	G	Analog ground
11	VOCM	A	Output common-mode voltage
12	VOUT	A	Analog Output
13	GND	G	Connect to GND
14	VDD	P	Connect to VDD
15	GND	G	Connect to GND
16	GND	G	Connect to GND

Table 11. Pin description of LMP91200

Temperature signal is analog signal, but the analog signal is very weak, so it is connected to operational amplifier OPA2317 and INA350. The circuit diagram is shown in Figure 23.

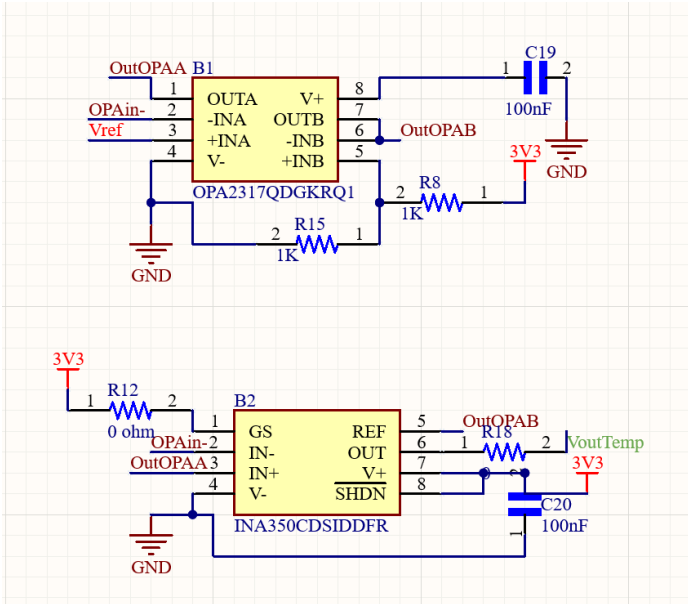

Fig. 25. Circuit diagram of OPA2317 and INA350

4.1.3 Microcontroller

The Microcontroller selected NINA-B3 series, Bluetooth 5 low energy modules. NINA-B3 series modules are small stand-alone Bluetooth 5 low energy modules featuring full Bluetooth 5 support, a powerful Arm Cortex-M4 with Float Point Unit (FPU), and state-of-the-art power performance. The embedded low power crystal improves power consumption by enabling optimal power save modes. NINA-B3 series modules are globally certified for use with the internal antenna or a range of external antennas. In many fields, NINA-B3 series is widely used, such as industrial automation, smart buildings and cities, low power sensors, wireless-connected and configurable equipment etc. Figure 26 shows the Block diagram of NINA-B3 series.

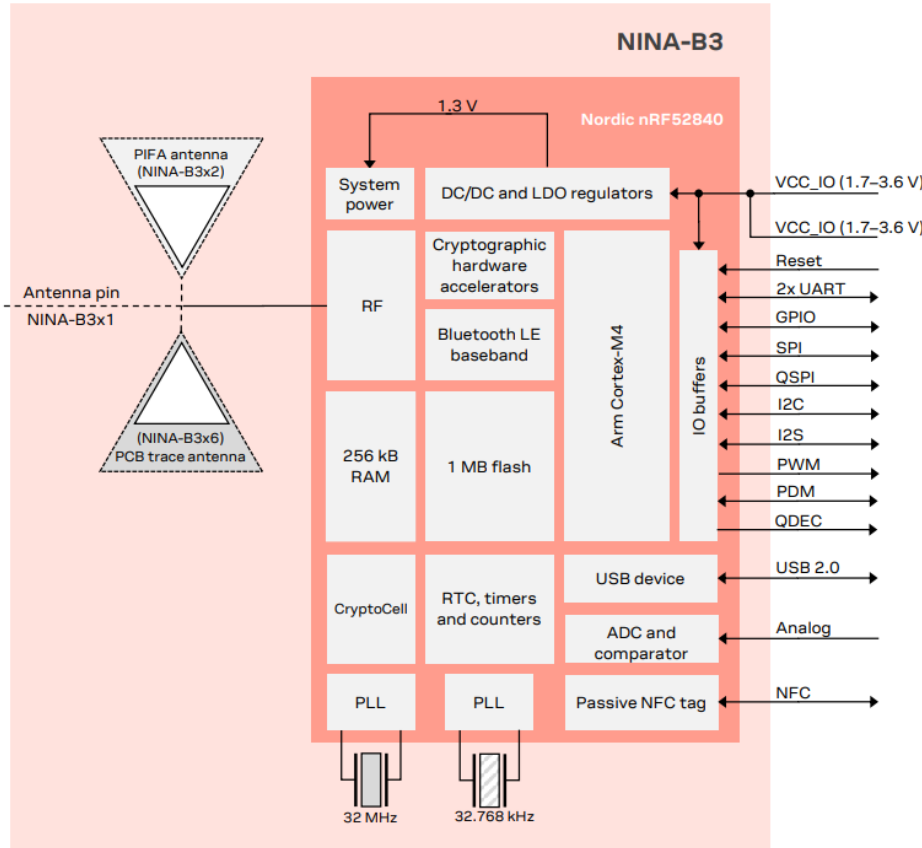

Fig. 26. Block diagram of NINA-B3 series

Figure 27 shows the circuit diagram of NINA-B3.

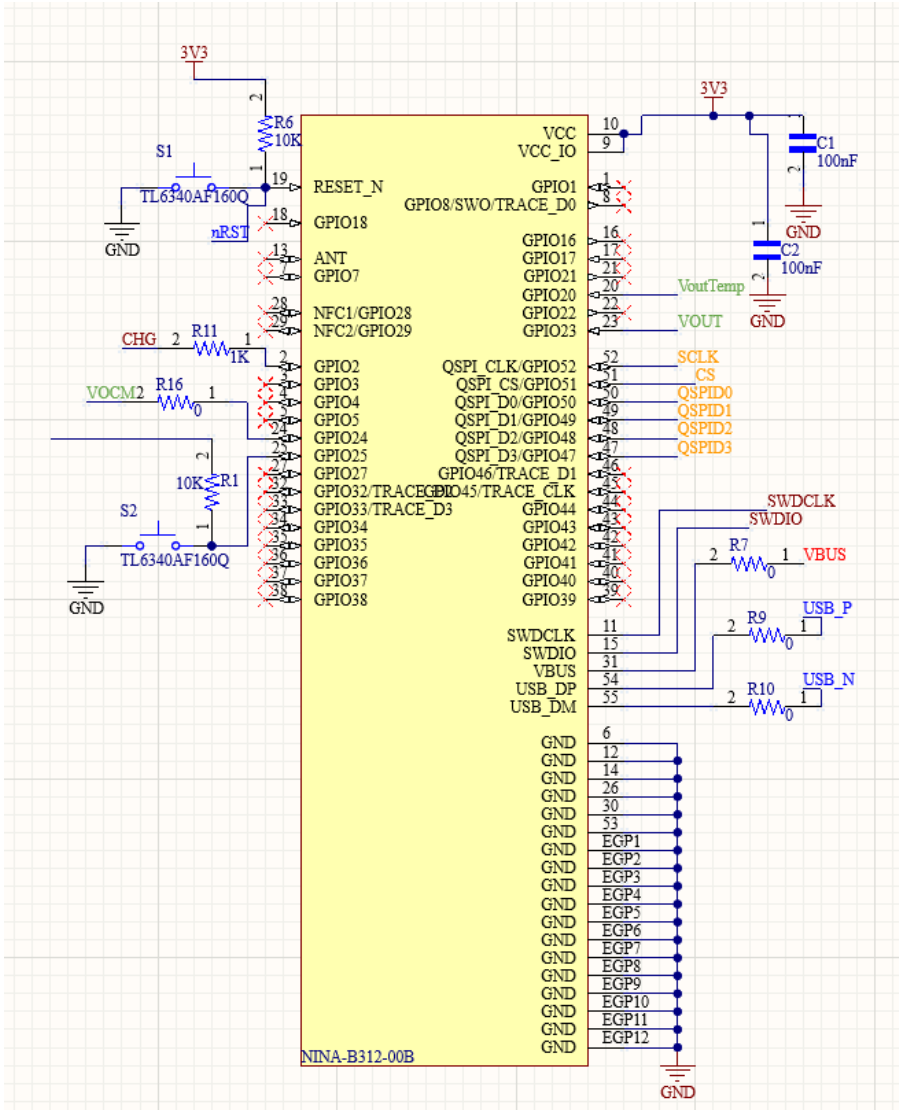

Fig. 27. Circuit Diagram of Microcontroller NINA-B3

4.2 Test software design

4.2.1 Test software platform environment

NINA-B3 series modules can be used either with the pre-flashed u-connectXpress software, or as an open CPU module in which you can run your own application developed with the Nordic SDK development environment inside the NINA-B3 module. The software on the NINA-B3 module contains the following parts:

1. SoftDevice S140 is a Bluetooth® Low Energy (LE) central and peripheral protocol stack solution
2. Optional bootloader
3. Application

NINA-B3 software structure and available software options are shown in Figure 28.

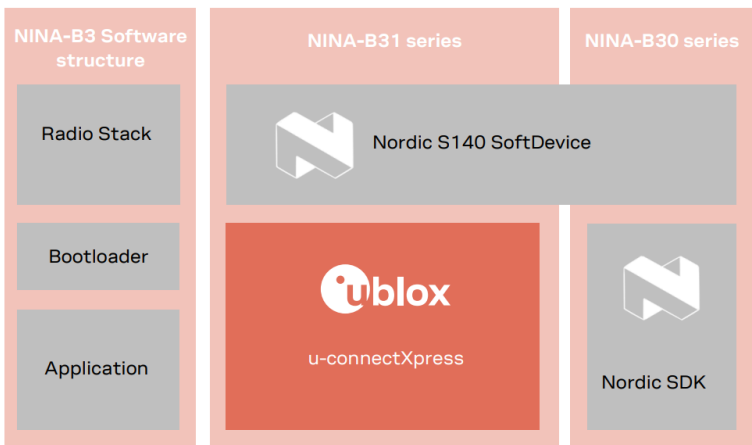

Fig. 28. NINA-B3 software structure and available software options

NINA-B31 series modules are delivered with the u-blox secure boot loader and pre-flashed u-connectXpress software. The u-connectXpress software enables use of the Bluetooth Low Energy functions, controlled by AT commands over the UART interface. Some of the supported features include the u-blox Low Energy Serial Port Service, GATT server and client, central and peripheral roles, and multidrop connections[17].

Figure 29 is the initial interface of u-connectXpress. You need to select the appropriate communication port, Boud rate and flow control, etc. Figure 30 is the u-connectXpress interface.

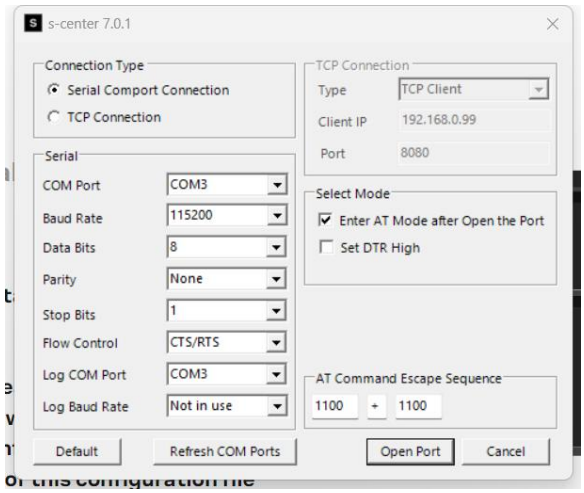

Fig. 29. u-connectXpress initial interface

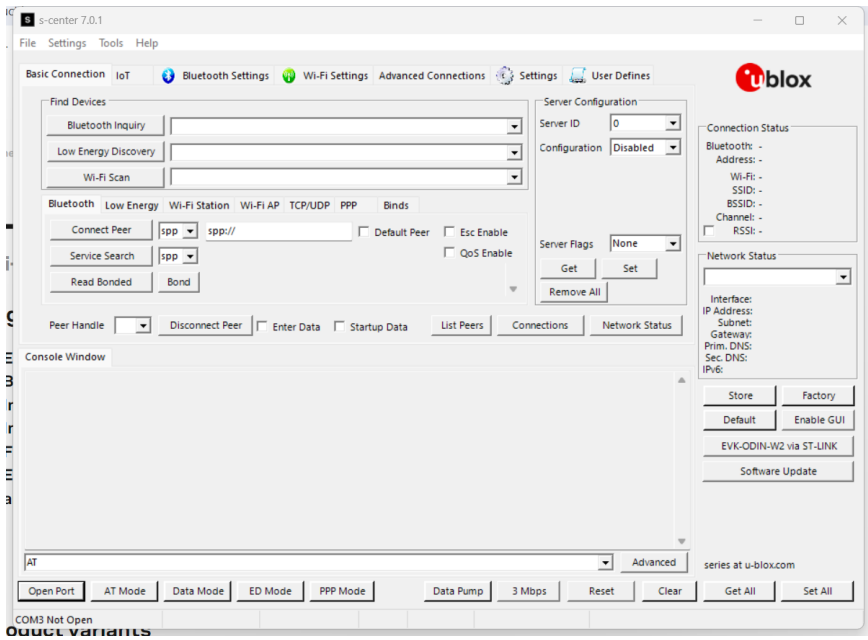

Fig. 30. u-connectXpress interface

4.2.2 Flashing

Before testing the PCB, the board needed to be flashed using J-Link. To build and define and flash, the nRF Connect SDK plugin in Visual Studio Code is used[18].

The serial port definition is shown in Figure 31.

```
#define NINA_RX       5   // P0.05 - GPIO23
#define NINA_TX       6   // P0.06 - GPIO22
#define NINA_SDA      16  // P0.16 - GPIO4
#define NINA_SCL      24  // P0.24 - GPIO5
//#define LED_DS1       7   // P0.07 - GPIO21
#define LED_RTS       31  // P0.31 - GPIO20
#define RGB_R         13  // P0.13 - GPIO1
#define RGB_G         25  // P0.25 - GPIO7 BOOT_I - *THIS PIN IS SHARED WITH SWITCH 1*
#define RGB_B         32  // P1.00 - GPIO8 SWO_I
#define B_SW1         25  // P0.25 - GPIO7 - SWITCH 1 - *THIS PIN IS SHARED WITH RGB GREEN*
#define B_SW2         2   // P0.02 - GPIO18 - SWITCH 2

#define CHG           14  // P0.14 - GPIO2 - Powersupply enable
#define VOCM          30  // P0.30 - GPIO24 - PHsensor output voltage
#define S2            4   // P0.04 - GPIO25 - switch2
#define SCLK          19  // P0.19 - GPIO52 - memory
#define CS            17  // P0.17 - GPIO51 - memory
#define QSPID0        20  // P0.20 - GPIO50 - memory
#define QSPID1        22  // P0.22 - GPIO49 - memory
#define QSPID2        21  // P0.22 - GPIO48 - memory
#define QSPID3        23  // P0.23 - GPIO47 - memory
```

Fig. 31. Serial port definition

4.3 Problems in the design

4.3.1 USB adapter battery charger invalid

Theoretically, with USB connected, but without DC power, MAX1555, the USB adapter battery charger can provide a constant voltage of 5V to V_{Bus} and charge the external battery. However, according to datasheet of MAX1555，charging current is related to DC voltage headroom ($V_{DC} - V_{Bat}$). Their relationship is shown in Figure 32.

The figure shows:

When $V_{DC} - V_{Bat} \geqslant$0.08V, there will be charge current.

When $V_{DC} - V_{Bat} \geqslant$0.22V, the charge current will become stable.

Typically, V_{Bat}=3.8V, therefore,

When $V_{DC} \geqslant$0.08V+V_{Bat}=3.88V, there will be charge current.

When $V_{DC} \geqslant$0.22V+V_{Bat}=4.08V, the charge current will become stable.

In the designed circuit connection of MAX1555, the designer decoupled DC with a 1μF ceramic capacitor to GND, so V_{DC} will not reach the expected value. As shown in Figure 33.

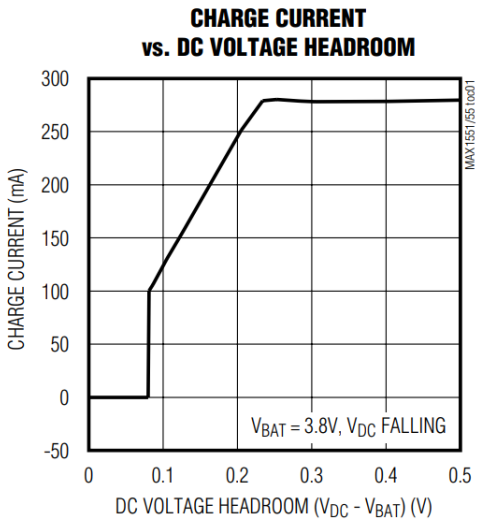

Fig. 32. DC Voltage Headroom VS. Charge Current

The USB and DC Input Selection provided by the Datasheet is shown in Table 12.

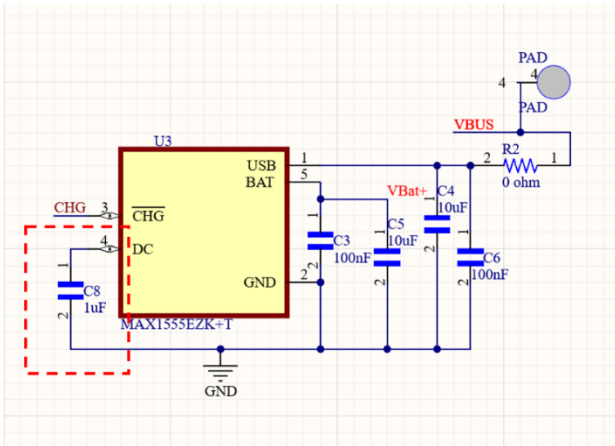

Fig. 33. MAX1555 decouple DC with capacitor to GND

V_{DC} > 7V OR V_{USB} > 6V	V_{DC} > 3.95V AND V_{USB} DON'T CARE	V_{DC} < 3.52V AND 3.95V < V_{USB} < 6V	V_{DC} AND V_{USB} < 3.52V
Exceeds operating input range. Not allowed. See the *Absolute Maximum Ratings* section.	280mA (typ) charging from DC	100mA (max) charging from USB	Undervoltage lockout

(V_{DC} takes precedence when both inputs are present.)

Table 12. USB and DC Input Selection

When V_{DC}＜3.52V, it must be powered by USB. However, after testing, the PCB was not successfully powered after the USB connector being connected to USB. The potentials of V_{Bus} and V_{Bat+}were still 0V, and then the potentials of V_{ref} and 3.3V power supply were also 0V. The reasons why this is the case will be explained later. Therefore, the power supply in the design cannot be used to provide voltage, and the PCB can only be powered by an external DC voltage source. The circuit diagram is shown in Figure 34. The 03 interface is connected to 3.3V and the 01 interface is connected to ground. The actual picture of the PCB is shown in Figure 35.

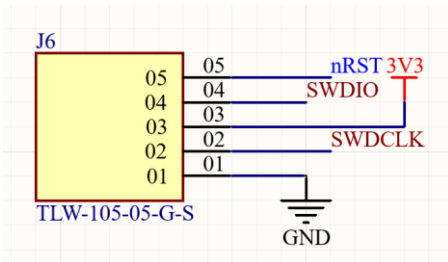

Fig. 34. Schematic of voltage supply connector

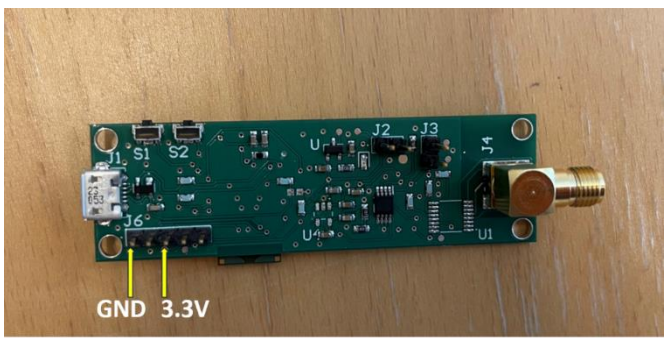

Fig. 35. Actual picture of the PCB with External 3.3V voltage source

4.3.2 Microcontroller Disconnected

After connecting the external 3.3V voltage source, the nodes on the PCB that should be 3.3V are tested, and they're all 3.3V, but there's no current flowing in the PCB. Generally speaking, there may be three reasons for no current flowing in the PCB[19]:

1. Open circuit: A connection in the circuit is broken, preventing current from flowing.
2. Short circuit: Two different nodes in the circuit are directly connected together, causing the current to bypass its intended path.
3. Isolation: Certain parts may be designed to be non-conductive, such as insulation layers or isolation devices, preventing the passage of electrical current.

First of all, after careful naked eye inspection, there is no obvious damage, detachment or unsoldered place on the wires, connectors and solder joints on the PCB board. Afterwards, a multimeter was used to measure the resistance between various nodes in the circuit, and there was no unexpected infinity resistance value or resistance that approaches zero infinitely, so the possibility of a short circuit or open circuit could be preliminarily ruled out.

After that, according to the necessity of each device in the circuit, the voltage regulator TPS70633, Voltage Reference REF3030, USB adapter battery charger MAX1555, operational amplifier OPA2317, operational amplifier INA350, FLASH memory MX25R803, sensor AFE LMP91200 were removed from the PCB in sequence using the hot air rework station as shown in Figure 36, and test whether there is current flowing in the PCB after each device is removed, and test the voltage of each node and the resistance value between different nodes. But the test results remained unchanged from before. Therefore, the possibility of isolation in the above devices can be preliminarily ruled out.

At this time, there is only one important device left on the PCB: the microcontroller. In order to determine whether the microcontroller is isolated, I directly added a voltage of 3.3V to the two poles of the coupling capacitor directly connected to the power supply node of the microcontroller. The PCB drawing of the voltage supply points are shown in Figure 37, and the points of PCB are shown in Figure 38.

Fig. 36. Hot air rework station

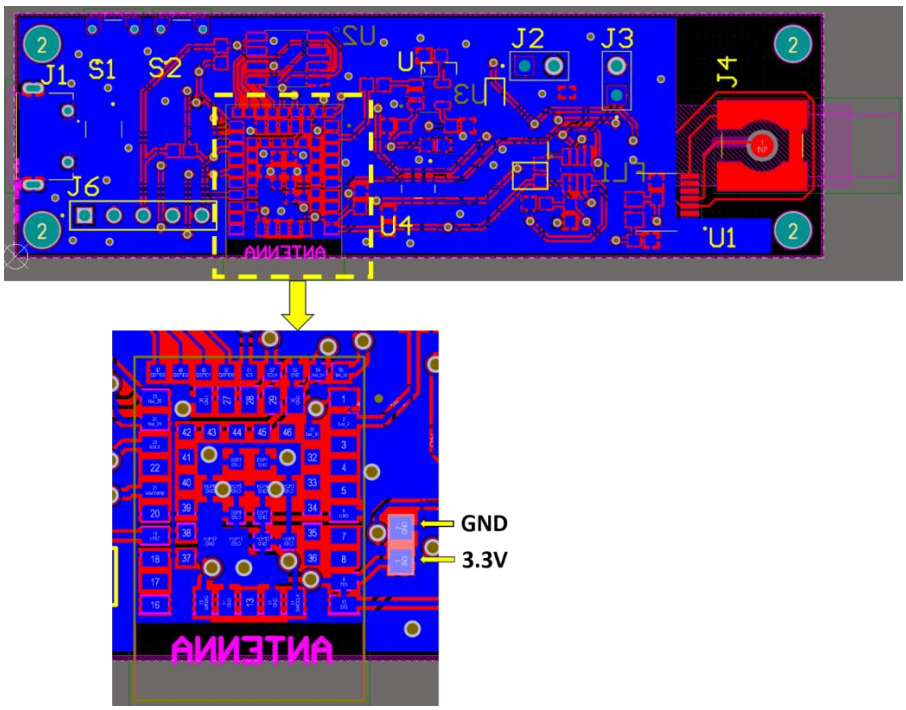

Fig. 37. Voltage supply point in PCB drawing

After directly applying 3.3V voltage to both ends of the microcontroller, there is still no current flowing in the PCB, so it is basically certain that the microcontroller is isolated.

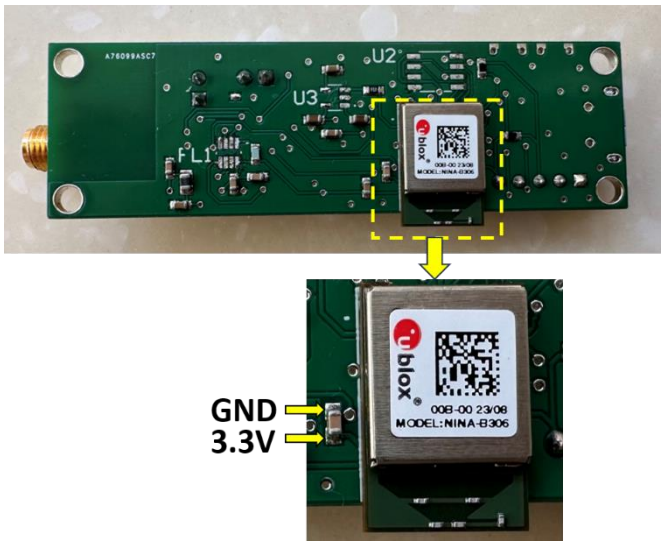

Fig. 38. Voltage supply point in PCB

Since the order quantity is less than ten pieces, manufacturers usually choose manual soldering instead of automatic soldering due to economic factors and time efficiency considerations. As shown in Figure 33, NINA-B3 is a Surface Mount Device (SMD). Manually soldering SMDs has a higher risk of failure as it is more susceptible to human factors[20].
Here are some possibilities and risks of failed manual soldering of SMDs:

1. Poor soldering: Manual soldering of SMD requires a high level of technical skills and experience. If the operation is not careful, it may lead to poor soldering, such as weak solder joints, solder bridging and other problems. This may affect the functional performance of the circuit or cause malfunction.
2. Component damage: When placing SMD components manually, if the placement is inaccurate or in the wrong direction, it may cause soldering failure or component damage. This may affect the circuit's connection performance or cause solder joints to short out.

3. Pin density: Complex SMD components usually have higher pin density, which means higher precision and stability are required when soldering. Soldering such a component manually can be more difficult because the solder joints are closer together and prone to solder misalignment or solder bridging.
4. Package size: Complex SMD components usually have smaller package sizes, which increases the difficulty of manual operation. Smaller package sizes can make components more susceptible to damage and require greater precision during placement and soldering.
5. Electrostatic discharge: SMD components are sensitive to static electricity. If static electricity is not properly handled and protected during manual welding, component damage or failure may occur.
6. Unstable soldering quality: The quality and consistency of manual soldering may be affected by the skill level of the operator, so the soldering quality may be unstable, making it difficult to guarantee the quality and reliability of each solder joint.

The NINA-B3 series selected for this design is prone to the above problems during manual soldering, resulting in surface mount failure. To sum up, I personally believe that the failure of this PCB to achieve the expected function is caused by the failure of manual soldering of the microcontroller.

As mentioned in 4.2.1, V_{Bus} and V_{Bat+} could not successfully supply proper voltage after the USB connector was connected to the USB, and it was still 0V is also because of this. As shown in Figure 21, the interfaces USB_P and USB_N of the USB connector are directly connected to the microcontroller, and the expected functions cannot be achieved when the microcontroller cannot operate normally.

5 Conclusions

In this thesis, I designed a water quality monitoring platform with a LoRa wireless transmission module, but due to cost issues and time issues, the design was not produced. In the testing part, I tried to test another water quality monitoring platform with Bluetooth functionality. After careful study and multiple attempts, the test failed and the board did not achieve the expected functionality. I explored possible issues with the board and eventually figured out why the board wasn't working properly. If my design can be manufactured, I can test the board.

6 Future work

If my design can be manufactured, I can test the board and further optimize the PCB design on the problems that arise during the test, so as to deepen my understanding of PCB design.

References

[1] https://www.marsden-weighing.co.uk/blog/what-is-total-body-water

[2] https://www.renkeer.com/top-7-water-quality-sensors/

[3] Racine, “Using Remote Sensing to Empower the Public to Address Water Pollution,” Wingspread Conference Center, September 2016

[4] Krikidis. S, Timotheou. S, Nikolaou, G. Zheng, D. W. K. Ng and R. Schober, "Simultaneous wireless information and power transfer in modern communication systems," in IEEE Communications Magazine, vol. 52, no. 11, pp. 104-110, Nov. 2014.

[5] S.F. Jilani, Q. H. Abbasi and A. Alomainy, "Inkjet-Printed Millimeter-Wave PET-Based Flexible Antenna for 5G Wireless Applications," 2018 IEEE MTT-S International Microwave Workshop Series on 5G Hardware and System Technologies (IMWS-5G), pp. 1-3, Dublin, Ireland, 2018.

[6] M. Jurčević and K. Malarić, "Assessment of Wi-Fi radiation on human health," 2016 24th International Conference on Software, Telecommunications and Computer Networks (SoftCOM), pp. 1-4, Split, Croatia, 2016.

[7] N. Kajikawa, Y. Minami, E. Kohno and Y. Kakuda, "On Availability and Energy Consumption of the Fast Connection Establishment Method by Using Bluetooth Classic and Bluetooth Low Energy," 2016 Fourth International Symposium on Computing and Networking (CANDAR), pp. 286-290, Hiroshima, Japan, 2016.

[8] G. Bhavana and K. M. Kumar, "Cardiac disease monitoring based on ZigBee technology," 2017 International Conference on Energy, Communication, Data Analytics and Soft Computing (ICECDS), pp. 392-395, Chennai, India, 2017.

[9] W. Chanwattanapong, S. Hongdumnuen, B. Kumkhet, S. Junon and P. Sangmahamad, "LoRa Network Based Multi-Wireless Sensor Nodes and LoRa Gateway for Agriculture Application," 2021 Research, Invention, and Innovation Congress: Innovation Electricals and Electronics (RI2C), pp. 133-136, Bangkok, Thailand, 2021.

[10] N. Mangalvedhe, R. Ratasuk and A. Ghosh, "NB-IoT deployment study for low power wide area cellular IoT," 2016 IEEE 27th Annual

International Symposium on Personal, Indoor, and Mobile Radio Communications (PIMRC), pp. 1-6, Valencia, Spain, 2016.

[11] B. X. Dai, "Research on Synchronization Method of Differential Protection Based on 5G Wireless Communication," 2021 International Conference on Power System Technology (POWERCON), pp. 2225-2228,Haikou, China, 2021.

[12] ZhiJiang. Zhou, Design and implementation of Ganjiang River water quality remote monitoring system based on STM32[D]. Nanchang University, 2022.DOI:10.27232/d.cnki.gnchu.2022.001784.

[13] https://blog.csdn.net/zhuimeng_ruili/article/details/103440507

[14] C. Zhao and Z. Hua, "Design of Motor Speed Control System Based on STM32 Microcontroller," 2022 International Conference on Computation, Big-Data and Engineering (ICCBE), pp. 274-276, Yunlin, Taiwan, 2022.

[15] Yin Y ,Xu H .Digital-intensive RFIC design techniques for transmitters in ISSCC 2023. ,44(04):12-13, Journal of Semiconductors,2023.

[16] Chang. Gao, Research on key technologies of underground comprehensive energy monitoring system based on LoRa communication [D]. Hebei University, 2021.

[17] V. A. Zyulin, I. A. Sterkhov, A. N. Semenova and I. I. Rastvorova, "Selection of Software and Hardware Components of Devices Designing a Mesh Network Using Bluetooth 5.1," 2022 Conference of Russian Young Researchers in Electrical and Electronic Engineering (ElConRus), pp. 101-105, Saint Petersburg, Russian Federation, 2022.

[18] Y. L. Xin, T. J. Yan, W. Schmitt, J. Nachreiner and C. L. May, "Pressureless low temperature sintering paste for NiAu PCB substrate," 2016 IEEE 18th Electronics Packaging Technology Conference (EPTC), pp. 584-588, Singapore, 2016.

[19] Charvaka Duvvury; Harald Gossner, "Soft Failure Mechanisms and PCB Design Measures," in System Level ESD Co-Design, pp.169-233, IEEE, 2015.

[20] https://www.seamarkzm.com/common-challenges-and-errors-in-manual-smd-reel-counting.html

Printed by Tryckeriet i E-huset, Lund 2024

LUND
UNIVERSITY

Series of Master´s theses
Department of Electrical and Information Technology
LU/LTH-EIT 2024-968
http://www.eit.lth.se